UDC 531.3:534.83:621.928:638.1
DOI: 10.15587/2706-5448.2026.353169

Yurii Syromiatnykov,
Oleksandr Bielykh,
Oleksandr Kharchenko

DEVELOPMENT OF AN ANALYTICAL MODEL FOR PREDICTING THE TRAJECTORY AND ENERGY DISSIPATION OF BEE BREAD GRANULES IN A ROTARY IMPACT SEPARATOR

The object of this research is the impact interaction between a bee bread granule and a hammer-type working element in a rotary separator. The practical relevance of the research arises from the need to ensure reliable release of granules while preventing their mechanical damage, since even partial destruction leads to deterioration of product quality and a decrease in its commercial value. Such an approach does not allow reliable prediction of energy transfer during impact or the subsequent trajectory of the granule. As a consequence, rotor speed and hammer mass are often selected without sufficient theoretical justification, which limits the efficiency and controllability of the separation process. To overcome these limitations, an analytical model describing granule impact and its post-impact motion in a rotating reference frame was developed. The mathematical formulation accounts for the combined action of centrifugal, Coriolis, gravitational, and friction forces, which made it possible to derive parametric relationships for velocity and displacement as functions of time. It was established that the post-impact motion follows a damped pattern, with the displacement amplitude decreasing by more than 60% within the first 0.02 s and exceeding an 80% reduction after 0.05 s. It was also found that energy transfer efficiency strongly depends on hammer mass. At a mass of 5 g, the efficiency reaches approximately 0.7–0.8%, whereas at 100 g it decreases to about 0.1%, and at 200 g it falls below 0.05%. These trends are explained by increasing dissipative losses within the rotating system. The proposed model enables prediction of granule trajectory, velocity, and energy dissipation under different operating conditions. Its practical value lies in providing a scientifically grounded basis for selecting hammer mass and rotor speed to achieve efficient and gentle separation of bee bread granules.

Keywords: *bee bread, granule, rotor, mechanics, inertia, energy, trajectory, separation, dissipation, efficiency.*

Received: 11.12.2025
Received in revised form: 05.02.2026
Accepted: 26.02.2026
Published: 28.02.2026

How to cite
Syromiatnykov, Y., Bielykh, O., Kharchenko, O. (2026). Development of an analytical model for predicting the trajectory and energy dissipation of bee bread granules in a rotary impact separator. Technology Audit and Production Reserves, 1 (1 (87)), 23–31. https://doi.org/10.15587/2706-5448.2026.353169

1. Introduction

Research on granular media traditionally relies on simplified mechanical models. These models are useful, but they rarely account for biological heterogeneity. Bee bread represents a granular system with internal porosity and variable material properties. In practice, its separation from wax combs inevitably involves impact interaction with rotating elements. The main difficulty is not only fragmentation. It is also the subsequent motion of the granule after impact. Impact penetration into granular beds has been described as a process of energy redistribution through compaction and rearrangement of particles [1]. Such results clarify general dissipation mechanisms, although they are mostly obtained for homogeneous systems. Rotation introduces additional mechanical effects. The behavior of soft porous bodies under rotational loading demonstrates that stress distribution depends on structural compliance [2]. This observation is relevant, but those models are not developed for repeated impact conditions. Interaction softness influences collective dynamics in particulate systems [3]. The implication is clear: contact mechanics cannot be neglected. At the same time, hydrodynamic effects may modify particle transport in flow-driven environments [4]. Therefore, motion in rotary devices cannot be interpreted as purely inertial. Contact duration and local deformation determine impulse transmission efficiency [5]. This is especially important for fragile materials. External excitation also reorganizes stress distribution inside particulate assemblies [6], although the direct connection between these stress changes and post-impact trajectory remains insufficiently clarified. Even a simplified two-particle collision model shows that motion after impact is governed by competition between translational energy and dissipation [7]. Impact experiments in granular beds confirm strong dependence on velocity and material properties [8]. However, these studies typically consider bulk layers rather than single granules interacting with moving tools. Granular rotor systems operate in nonequilibrium regimes under continuous rotation [9]. In industrial crushers, rotor-induced airflow alters fragmentation intensity [10]. Numerical simulations demonstrate that rotor geometry affects circulation and residence time [11]. Experimental analysis of hammer elements confirms that configuration parameters determine load distribution [12]. Structural optimization improves stability and wear resistance [13]. Yet, an analytical link between geometry and particle-scale trajectory is still lacking. Design investigations of rotor-based systems show that impact and rotation act simultaneously [14]. Productivity of hammer mills depends strongly on operating parameters [15]. Dissipative mechanisms due to friction and internal deformation dominate post-impact evolution [16]. Repeated collisions accelerate attenuation of kinetic energy [17]. In hammer systems, concave geometry affects breakage intensity [18], and degradation results from combined impact and shear [19]. Discrete element simulations confirm the influence of velocity and contact configuration on fragmentation probability [20]. Transport and separation remain central engineering problems [21]. Machine stability affects material flow behavior [22]. Transporting

ISSN-L 2664-9969; E-ISSN 2706-5448

capability determines technological efficiency [23]. Rotor geometry and kinematic parameters govern controlled motion in rotary mechanisms [24]. Thus, although experimental and numerical investigations are numerous, a consistent analytical description of post-impact motion of structurally fragile biological granules in rotary systems has not been sufficiently developed. This limitation complicates the rational selection of operating parameters for bee bread separation.

The object of research is the process of impact interaction between a bee bread granule and a rotating working element of a rotary separator.

The aim of research is to develop an analytical model describing impact interaction and post-impact motion of a bee bread granule in a rotary separation system.

Research objectives:

1. To derive analytical relationships describing the post-impact motion of a bee bread granule.
2. To determine the influence of impact parameters and rotor operating conditions on energy dissipation and particle trajectory.

2. Materials and Methods

The object considered is a single bee bread granule interacting with a hammer element inside a rotary impact device. The granule is treated as a soft deformable particle, which is consistent with common modeling approaches for biological and viscoelastic materials under impact and compression [1–3, 19]. Bee bread granules, formed through natural fermentation and characterized by internal heterogeneity, can exhibit a combined elastic–plastic response with pronounced damping, comparable in a general mechanical sense to soft porous spheres and biological composites discussed in the literature [2, 3, 6].

The methodology is based on analytical mechanics. To represent the actual operating environment of a rotary device, the motion is described in a non-inertial Cartesian coordinate system rigidly attached to the rotating frame. This formulation allows centrifugal and Coriolis terms to enter the equations of motion explicitly, rather than being introduced as secondary corrections [2, 4, 9, 11, 16]. Such a choice is standard in modern studies of particle motion in rotating systems, where rotation can alter trajectories and dissipation mechanisms even when the contact event itself is short [4, 9, 10].

The contact interaction between the granule and the hammer is represented using an impulse-based formulation consistent with nonlinear contact mechanics for deformable particles [1, 7, 8]. The normal contact force is written through a nonlinear stiffness–damping relation, capturing both deformation during compression and partial recovery after unloading, as is typical in soft-particle impact models and discrete element approaches [1, 3, 19]. Tangential interaction is described using the Coulomb friction law with a constant coefficient of friction, which provides a transparent and widely used baseline for impact systems involving sliding at contact [5, 12, 15].

After the contact stage, the granule is assumed to move freely within the rotating frame under the combined action of inertial forces, gravity, and frictional resistance. The post-impact motion is reduced to a second-order non-homogeneous differential equation for the displacement along the radial direction of the rotating coordinate system. Analytical solutions are obtained using the method of variation of parameters, and the resulting expressions are used to discuss trajectories both in the rotating frame and in an inertial frame for interpretation [2, 4, 10, 14]. This approach follows established treatments of particle–rotor dynamics and granular motion in rotating environments [10, 11, 13, 20].

Symbolic verification of derived relations and numerical checks, together with visualization of key dynamic quantities, are performed in Mathcad 15 (PTC Inc., USA) and Statistica 10.0 (StatSoft Inc., USA). The model assumes uniform rotor angular velocity, and the impact is treated as a short-duration event, which supports a quasi-static approximation during the contact interval – an assumption commonly used in analytical descriptions of rotary impact mechanisms when the goal is to obtain interpretable parametric dependencies [10, 12, 13, 17]. To keep the formulation analytically tractable while retaining the essential kinematics, the hammer–rotor geometry is simplified; at the same time, the relationships required to represent the impact conditions and the subsequent motion are preserved. Overall, the modeling strategy combines elements of soft-particle mechanics, impact theory, and rotating-frame dynamics in a form suitable for engineering analysis and design-oriented optimization of rotary processing systems for biological granular materials [19–24].

3. Results and Discussion

3.1. Post-impact motion, trajectory, and velocity of the bee bread granule

It is possible to consider the motion of a bee bread granule inside the working chamber of a rotary system immediately after its detachment from the wax matrix, caused by impulse-contact interaction with a hammer element. In the adopted formulation, the impact phase determines the initial conditions for the granule's motion, which is further analyzed in a non-inertial coordinate system *Oxyz* rigidly attached to the uniformly rotating rotor.

Additional contacts of the granule with chamber walls are neglected; only the motion in the field of inertial forces and in the contact zone with the hammer surface is considered (Fig. 1).

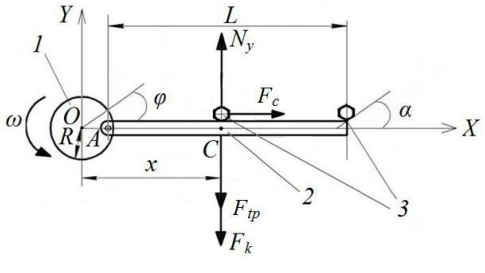

Fig. 1. Schematic diagram of forces acting on the bee bread granule in the contact zone with the hammer (top view): 1 – rotor, 2 – hammer, 3 – granule

The rotor rotates in a horizontal plane with constant angular velocity ω. The granule of mass m undergoes translational motion with the rotor and relative motion along the x-axis of the rotating coordinate system. Since the rotation is uniform, it is possible to assume quasi-static behavior along the y-axis, taking acceleration in that direction as zero. The force balance along the y and z axes is used to derive the normal reactions.

The system of equations describing the relative motion of the granule is written as

$$\begin{cases} m\ddot{x} = F_c - F_k - F_{tp}, \\ F_c = m\omega^2 x, \\ F_k = 2m\omega\dot{x}, \\ F_{tp} = fmg, \end{cases} \quad (1)$$

where $x(t)$ – the relative displacement of the granule; F_{tp} – the dry friction force in the contact zone "granule-hammer"; F_c – the centrifugal force; F_k – the Coriolis force; f – the coefficient of friction; ω – the angular velocity; g is the gravitational acceleration.

The centrifugal force in the rotating coordinate system is expressed as

$$F_c = m\omega^2 x. \quad (2)$$

The Coriolis force arising due to relative velocity is given by

$$F_k = 2m\omega\dot{x}, \tag{3}$$

where ω – the angular velocity of the rotor and $\dot{x}$ – the relative velocity of the granule along the x-axis.

From the second equation in system (1), considering equation (3), it is possible to obtain the normal reaction along the y-axis explicitly as

$$N_y = F_k = 2m\omega\dot{x}, \tag{4}$$

where N_y – the normal reaction force, m – the mass of the granule, g – the gravitational acceleration, and ω and $\dot{x}$ as defined earlier.

The dry friction force in the contact zone is modeled using Coulomb's law with friction coefficient f, written in an expanded form to preserve the link with inertial components

$$F_{tp} = fmg. \tag{5}$$

Substituting equations (2) and (5) into the first equation of system (1), it is possible to obtain the equation of motion in the form

$$m\ddot{x} = 2mf\omega\dot{x} - m\omega^2 x, \tag{6}$$

where the right-hand side combines centrifugal acceleration, gravity, and velocity-dependent friction.

Using the geometric identification of radial coordinate as $r = x$, it is possible to simplify (6) to

$$m\ddot{x} + 2mf\omega\dot{x} - m\omega^2 x = fmg. \tag{7}$$

Dividing equation (7) by the nonzero mass mmm, it is possible to obtain the final form of the relative motion equation

$$\ddot{x} + 2f\omega\dot{x} - \omega^2 x = fg, \tag{8}$$

where $\ddot{x}$ represents the granule acceleration in the rotating frame; the term $2f\omega\dot{x}$ characterizes dissipative effects associated with friction and the Coriolis interaction; and the term $\omega^2 x$ corresponds to the centrifugal inertial component acting on the granule. To analyze the dynamics of the granule's post-impact motion in the rotating system, it is possible to solve equation (8) as a linear non-homogeneous differential equation with constant coefficients. The associated homogeneous equation

$$\ddot{x} + 2f\omega\dot{x} - \omega^2 x = 0,$$

yields the characteristic equation

$$\lambda^2 + 2f\omega\lambda - \omega^2 = 0. \tag{9}$$

The discriminant of the characteristic equation is given explicitly as

$$D = (2f\omega)^2 + 4\omega^2 = 4\omega^2(f^2 + 1), \tag{10}$$

where $\Delta = (2f\omega)^2 + 4\omega^2$ defines the type of solution (overdamped, underdamped, or critically damped).

Solving the characteristic equation, it is possible to obtain the roots

$$\lambda_{1,2} = \frac{-2f\omega \pm \sqrt{D}}{2} = -f\omega \pm \omega\sqrt{f^2+1}, \tag{11}$$

where λ_1 and λ_2 – the exponential rates of decay or growth, depending on the sign of the real parts. These roots define the fundamental modes of the system.

Accordingly, the general solution of the homogeneous equation can be written in the exponential form

$$x_0(t) = C_1 e^{\lambda_1 t} + C_2 e^{\lambda_2 t}, \tag{12}$$

where C_1 and C_2 – arbitrary constants to be determined from initial conditions; λ_1, λ_2 are the roots obtained from equation (11); and $x_0(t)$ is the homogeneous part of the solution.

This solution captures the damped oscillatory behavior or exponential decay of the granule's displacement in the absence of external forcing.

To construct the complete solution of the non-homogeneous differential equation (8), it is possible to apply the method of variation of constants (variation of parameters), retaining the exponential basis $\left\{e^{\lambda_1 t}, e^{\lambda_2 t}\right\}$.

The particular solution is represented in the form

$$x_p(t) = u_1(t)e^{\lambda_1 t} + u_2(t)e^{\lambda_2 t}, \tag{13}$$

where $x_p(t)$ – the particular solution, and $u_1(t)$, $u_2(t)$ – unknown functions replacing the constants C_1, C_2 in the homogeneous solution.

According to the method of variation of constants, the derivatives of $u_1(t)$, $u_2(t)$ satisfy the following system

$$\begin{cases} u_1'(t)e^{\lambda_1 t} + u_2'(t)e^{\lambda_2 t} = 0, \\ u_1'(t)\lambda_1 e^{\lambda_1 t} + u_2'(t)\lambda_2 e^{\lambda_2 t} = -f^2 g, \end{cases} \tag{14}$$

where the non-homogeneous term is formally expressed through a generalized loading parameter fg, and the fundamental system is $\left\{e^{\lambda_1 t}, e^{\lambda_2 t}\right\}$.

The Wronskian of the fundamental system is computed as

$$W(t) = \begin{vmatrix} e^{\lambda_1 t} & e^{\lambda_2 t} \\ \lambda_1 e^{\lambda_1 t} & \lambda_2 e^{\lambda_2 t} \end{vmatrix} = (\lambda_2 - \lambda_1)e^{(\lambda_1+\lambda_2)t}, \tag{15}$$

where $W(t)$ – the determinant of the matrix composed of fundamental solutions and their derivatives.

Given the exponential nature of the basis, there is the equivalent form

$$W(t) = 2\omega\sqrt{f^2+1}\, e^{-2f\omega t}, \tag{16}$$

which simplifies the computation of the integrals in the next step.

From expressions (14)–(16), the derivatives of the variable coefficients are obtained as

$$u_1'(t) = \frac{fge^{\lambda_2 t}}{W(t)}, \tag{17}$$

and

$$u_2'(t) = -\frac{fge^{\lambda_1 t}}{W(t)}, \tag{18}$$

where u_1' and u_2' represent the rates of variation of constants corresponding to each fundamental mode.

Substituting equation (16) into (17)–(18), it is possible to obtain integrable expressions for the unknown functions

$$u_1'(t) = \frac{fg}{2\omega\sqrt{f^2+1}} e^{(\lambda_2+2f\omega)t}, \tag{19}$$

and

$$u_2'(t) = -\frac{fg}{2\omega\sqrt{f^2+1}} e^{(\lambda_1+2f\omega)t}, \tag{20}$$

ISSN-L 2664-9969; E-ISSN 2706-5448

where the exponential denominators reflect the influence of the dynamic damping terms.

Integrating the expressions in (19), (20)

$$u_1(t)=\frac{fg}{2\omega\sqrt{f^2+1}}\cdot\frac{e^{(\lambda_2+2f\omega)t}}{\lambda_2+2f\omega}, \quad (21)$$

and

$$u_2(t)=-\frac{fg}{2\omega\sqrt{f^2+1}}\cdot\frac{e^{(\lambda_1+2f\omega)t}}{\lambda_1+2f\omega}, \quad (22)$$

where the integration constants can be omitted, as they are already included in the homogeneous part of the general solution.

Finally, substituting equations (21), (22) into expression (13), it is possible to obtain the particular solution in explicit form

$$x_p(t)=u_1(t)e^{\lambda_1 t}+u_2(t)e^{\lambda_2 t}. \quad (23)$$

Multiplying out the exponentials, the full expression is conveniently rewritten in a format that matches the structure of the original derivation

$$x(t)=C_1e^{\lambda_1 t}+C_2e^{\lambda_2 t}-\frac{fg}{\omega^2}. \quad (24)$$

Applying the initial condition at the moment of separation $t_0 = 0$, where the granule has displacement $x(0) = x_0$, it is possible to substitute this into expression (24) and obtain

$$x(0)=x_0\Rightarrow C_1+C_2-\frac{fg}{\omega^2}=x_0. \quad (25)$$

From this, it is possible to isolate the constant of integration

$$C_2=x_0+\frac{fg}{\omega^2}-C_1, \quad (26)$$

where x_0 – the initial displacement of the granule after impact; this constant defines the amplitude of the motion.

Substituting equation (26) into (24), it is possible to obtain the final analytical expression for the post-impact displacement of the granule in the contact zone

$$x(t)=C_1e^{\lambda_1 t}+\left(x_0+\frac{fg}{\omega^2}-C_1\right)e^{\lambda_2 t}-\frac{fg}{\omega^2}, \quad (27)$$

where $x(t)$ – the radial displacement of the granule in the rotating coordinate system, expressed as a decaying function of time due to the damping effect of friction and inelastic impact losses.

For uniform rotor rotation, the angular displacement over time is defined by the simple kinematic relationship

$$\varphi(t)=\varphi_0+\omega t, \quad (28)$$

where $\varphi(t)=\omega t+\varphi_0$ – the angular position of the rotor at time t; ω – the constant angular velocity; φ_0 – the angular phase at the moment of impact.

Thus, the radial displacement of the granule in the rotating coordinate system is given in a parametric form, convenient for trajectory reconstruction

$$r(t)=R+x(t), \quad (29)$$

where $r(t)$ corresponds to the radial coordinate of the granule, which is identical to the displacement $x(t)$ in the rotating coordinate system.

To describe the motion of the granule in the fixed (laboratory) frame, it is possible to convert from the rotating coordinate system $Oxyz$ to the horizontal plane OXY. The transformation leads to the following parametric trajectory equations

$$X(t)=(R+x(t))\cos\varphi(t), \quad (30)$$

and

$$Y(t)=(R+x(t))\sin\varphi(t), \quad (31)$$

$$\begin{cases}X(t)=(R+x(t))\cos(\varphi_0+\omega t),\\ Y(t)=(R+x(t))\sin(\varphi_0+\omega t),\end{cases} \quad (32)$$

where $X(t)$, $Y(t)$ – the coordinates of the granule in the stationary system; $r(t)$ – the radial displacement obtained from equation (29); $\varphi(t)$ – the angular displacement defined in (28).

Using the parametric relations (30)–(32), the trajectory of the granule in the coordinate system was reconstructed. The resulting space–time representation of motion and its planar projection are shown in Fig. 2. As can be seen, the granule follows a strongly curved, spiral-like path with a rapidly decreasing radial amplitude, which reflects the combined action of inertial forces and intensive energy dissipation after impact. The color-coded time distribution along the trajectory demonstrates that the main part of the displacement occurs within a very short time interval, while the subsequent motion is characterized by rapid deceleration and convergence toward the rotor center. This confirms that the post-impact dynamics of the granule is highly non-uniform in time and dominated by dissipative effects.

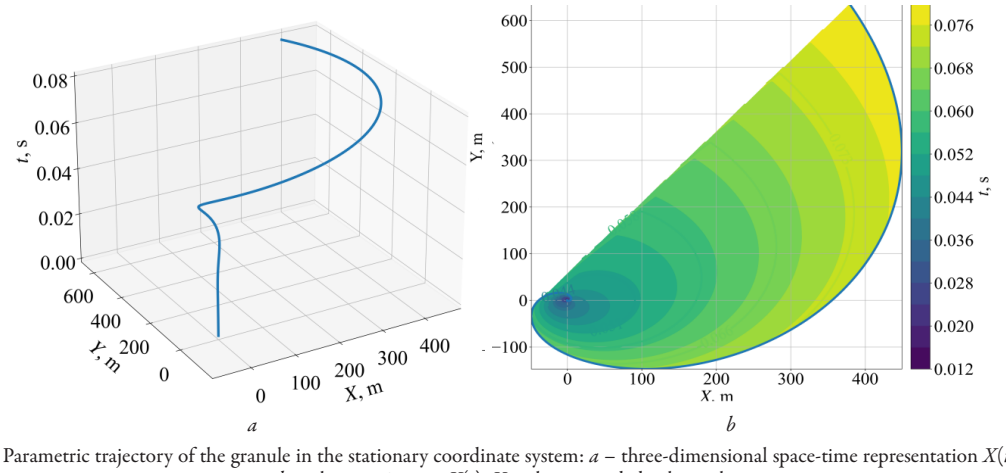

Fig. 2. Parametric trajectory of the granule in the stationary coordinate system: *a* – three-dimensional space-time representation $X(t)$, $Y(t)$; *b* – planar trajectory $X(t)$, Y with time-coded color scale

These expressions allow the reconstruction of the granule's path in space as a time-dependent spiral-like curve with damping amplitude.

To evaluate the transport intensity, it is possible to define the modulus of the granule's velocity vector as

$$V(t)=\sqrt{\dot{X}(t)^2+\dot{Y}(t)^2}. \quad (33)$$

Since $\varphi(t)=\omega t+\varphi_0$, its derivative with respect to time is

$$\dot{\varphi}(t)=\omega,\ \ddot{\varphi}(t)=0, \quad (34)$$

where ω – the constant rotor speed.

By differentiating equations (30) and (31) with respect to time and substituting from (34), it is possible to obtain the explicit components of velocity

$$\begin{cases}\dot{X}(t)=\dot{x}(t)\cos(\varphi_0+\omega t)-\omega(R+x(t))\sin(\varphi_0+\omega t),\\ \dot{Y}(t)=\dot{x}(t)\sin(\varphi_0+\omega t)+\omega(R+x(t))\cos(\varphi_0+\omega t),\end{cases} \quad (35)$$

where $\dot{x}(t)$ represents the time derivative of the radial displacement; ω is the angular velocity of the rotor; and the sine and cosine functions define the geometric transformation of radial and circumferential velocity components from the rotating frame to the stationary coordinate system OXY.

To evaluate $\dot{r}(t)$, it is possible to differentiate equation (29) and write

$$\dot{x}(t)=\lambda_1 C_1 e^{\lambda_1 t}+\lambda_2\left(x_0+\frac{fg}{\omega^2}-C_1\right)e^{\lambda_2 t}. \quad (36)$$

Substituting (35) into (33) and applying trigonometric identities, it is possible to obtain a time-invariant expression for the velocity magnitude

$$V^2(t)=\dot{X}(t)^2+\dot{Y}(t)^2. \quad (37)$$

After expanding and regrouping the squares and mixed terms, it is possible to find

$$\begin{aligned}V^2(t)=&\dot{x}^2(t)\cos^2(\varphi_0+\omega t)-\\&-2\omega x(t)\dot{x}(t)\sin(\varphi_0+\omega t)\cos(\varphi_0+\omega t)+\\&+\omega^2x^2(t)\sin^2(\varphi_0+\omega t)+\dot{x}^2(t)\sin^2(\varphi_0+\omega t)+\\&+2\omega x(t)\dot{x}(t)\sin(\varphi_0+\omega t)\cos(\varphi_0+\omega t)+\\&+\omega^2x^2(t)\cos^2(\varphi_0+\omega t).\end{aligned} \quad (38)$$

The mixed terms cancel due to orthogonality, and using the identity

$$\sin^2\theta+\cos^2\theta=1,\ \theta=\varphi_0+\omega t, \quad (39)$$

it is possible to arrive at the final invariant form of velocity

$$V^2(t)=\dot{x}(t)^2+\omega^2(R+x(t))^2. \quad (40)$$

Using expression (40), the maximum attainable velocity of the granule was evaluated in a wide range of rotor angular velocities ω and friction coefficients f. The resulting parametric dependence $v_{max}(\omega,f)$ is shown in Fig. 3. It can be seen that the maximum velocity increases sharply with increasing ω and decreasing f, forming a strongly nonlinear response surface. This demonstrates the high sensitivity of the impact kinematics to both rotor speed and contact friction conditions.

The results shown in Fig. 4 demonstrate that with increasing hammer mass, the efficiency of energy transfer to the granule decreases sharply. At a hammer mass of 5 g, efficiency is around 0.7–0.8%; at 100 g, it drops to approximately 0.1%; and at 200 g, to below 0.05%. This confirms the inelastic nature of impact and suggests the presence of an optimal mass for maximum energy utilization.

The trajectories demonstrate rapidly decaying oscillations caused by strong internal dissipation and inelastic losses during impact and subsequent motion.

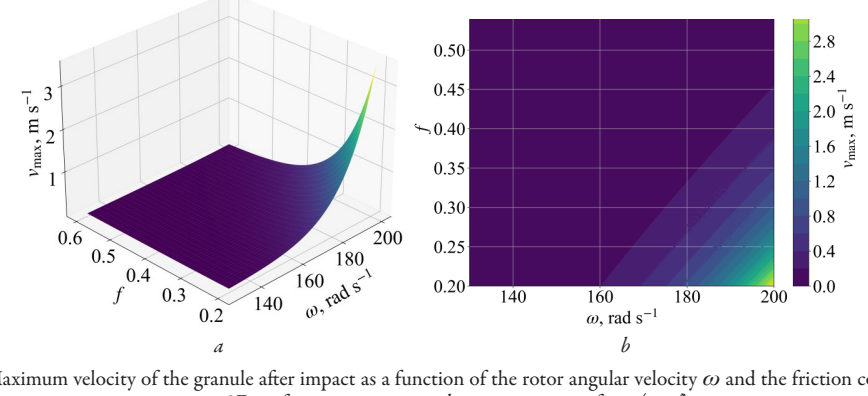

Fig. 3. Maximum velocity of the granule after impact as a function of the rotor angular velocity ω and the friction coefficient f: *a* – 3D surface representation; *b* – contour map of $v_{max}(\omega, f)$

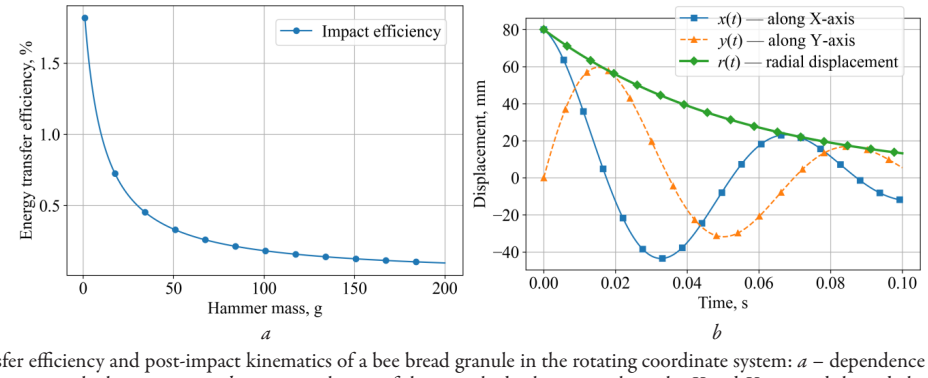

Fig. 4. Energy transfer efficiency and post-impact kinematics of a bee bread granule in the rotating coordinate system: *a* – dependence of the impact energy transfer efficiency on the hammer mass; *b* – time evolution of the granule displacement along the X and Y axes and the radial coordinate $r(t)$

ISSN-L 2664-9969; E-ISSN 2706-5448

The granule's displacement exhibits exponentially decaying behavior. For an initial deviation of 80 mm, the amplitude drops by over 60% within 0.02 s and by more than 80% within 0.05 s. The radial component $r(t)$ decreases monotonically from ≈80 mm to less than 20 mm in the same interval, indicating rapid dissipation and a short-lived dynamic phase.

3.2. Influence of impact and operating parameters on granule motion and energy dissipation

To fully characterize the motion of the hammer and its interaction with the bee bread granule, it is possible to formulate the kinematics in terms of generalized coordinates and velocities.

The generalized coordinate vector of the system is given by

$$\mathbf{q}(t)=\begin{cases}\varphi(t),\\ \alpha(t),\end{cases} \tag{41}$$

where $\varphi(t)$ – the angular position of the rotor; $\alpha(t)$ – the angular displacement of the hammer relative to the radial direction of the rotor; t is time.

The generalized velocities and accelerations are expressed as

$$\dot{\mathbf{q}}(t)=\begin{cases}\dot{\varphi}(t),\\ \dot{\alpha}(t),\end{cases}\ \ddot{\mathbf{q}}(t)=\begin{cases}\ddot{\varphi}(t),\\ \ddot{\alpha}(t),\end{cases} \tag{42}$$

where $\dot{\varphi}(t)$ and $\ddot{\varphi}(t)$ – the first and second time derivatives of the rotor angular position, respectively; $\dot{x}(t)$ and $\ddot{x}(t)$ are the first and second time derivatives of the hammer angular displacement; t is time.

The position of the hammer's pivot point A, located at radius R, in the fixed coordinate system OXY, is given by

$$\mathbf{r}_A(t)=\begin{cases}R\cos\varphi(t),\\ R\sin\varphi(t),\end{cases} \tag{43}$$

where $\varphi(t)=\omega t+\varphi_0$ – the angular position of the rotor, as defined earlier.

The velocity and acceleration of point A are computed as

$$\dot{\mathbf{r}}_A(t)=\begin{cases}-R\dot{\varphi}(t)\sin\varphi(t),\\ R\dot{\varphi}(t)\cos\varphi(t),\end{cases} \tag{44}$$

and

$$\ddot{\mathbf{r}}_A(t)=\begin{cases}-R\ddot{\varphi}(t)\sin\varphi(t)-R\dot{\varphi}^2(t)\cos\varphi(t),\\ R\ddot{\varphi}(t)\cos\varphi(t)-R\dot{\varphi}^2(t)\sin\varphi(t),\end{cases} \tag{45}$$

where the radial direction and its orthogonal complement define the local basis for expressing linear quantities in the rotating frame.

To analyze the hammer's motion in full, it is possible to define the position of its center of mass C, which is located a distance L from point A, and depends on the relative angular position $\alpha(t)$

$$\mathbf{r}_C(t)=\mathbf{r}_A(t)+L\begin{cases}\cos\big(\varphi(t)+\alpha(t)\big),\\ \sin\big(\varphi(t)+\alpha(t)\big),\end{cases} \tag{46}$$

where L – the length from the joint to the center of mass.

The velocity of point C is then derived from equation (46)

$$\dot{\mathbf{r}}_C(t)=\dot{\mathbf{r}}_A(t)+L\big(\dot{\varphi}(t)+\dot{\alpha}(t)\big)\begin{cases}-\sin\big(\varphi(t)+\alpha(t)\big),\\ \cos\big(\varphi(t)+\alpha(t)\big).\end{cases} \tag{47}$$

The square of the center of mass velocity is expressed in expanded form as

$$v_C^2(t)=R^2\dot{\varphi}^2(t)+L^2\big(\dot{\varphi}(t)+\dot{\alpha}(t)\big)^2+$$
$$+2RL\,\dot{\varphi}(t)\big(\dot{\varphi}(t)+\dot{\alpha}(t)\big)\cos\alpha(t). \tag{48}$$

After simplification and grouping of terms, let's arrive at an equivalent expression: (48) (repeated with reduced notation).

To formulate the impact law, it is necessary to determine the velocity components of the hammer surface at the contact point with the granule.

The position of the contact point K on the hammer is determined as

$$\mathbf{r}_K(t)=\mathbf{r}_A(t)+a\begin{cases}\cos\big(\varphi(t)+\alpha(t)\big),\\ \sin\big(\varphi(t)+\alpha(t)\big),\end{cases} \tag{49}$$

where A – the hinge point of the hammer (from (43)); a – the distance from point A to the contact point K along the hammer's axis; $\alpha(t)$ – the angular position of the hammer.

Substituting from equation (43), it is possible to obtain the explicit coordinates of K

$$\begin{cases}x_K(t)=R\cos\varphi(t)+a\cos\big(\varphi(t)+\alpha(t)\big),\\ y_K(t)=R\sin\varphi(t)+a\sin\big(\varphi(t)+\alpha(t)\big).\end{cases} \tag{50}$$

Differentiating with respect to time, the velocity of point K is given by

$$\dot{\mathbf{r}}_K(t)=\dot{\mathbf{r}}_A(t)+a\big(\dot{\varphi}(t)+\dot{\alpha}(t)\big)\begin{cases}-\sin\big(\varphi(t)+\alpha(t)\big),\\ \cos\big(\varphi(t)+\alpha(t)\big),\end{cases} \tag{51}$$

where $\dot{\varphi}(t)=\omega$ is the angular speed of the rotor; $\dot{\alpha}(t)$ is the angular velocity of the hammer relative to the rotor.

Squaring the velocity vector

$$v_K^2(t)=\dot{\mathbf{r}}_K(t)\cdot\dot{\mathbf{r}}_K(t)=\dot{x}_K^2(t)+\dot{y}_K^2(t), \tag{52}$$

which expresses the total kinetic energy of the contact point before interaction.

To determine the interaction mechanics, it is possible to extract the normal component of the contact velocity. Assuming that the hammer surface is locally perpendicular to the radial direction, it is possible to define the normal direction and compute the projection:

$$\mathbf{n}(t)=\begin{cases}\cos\big(\varphi(t)+\alpha(t)\big),\\ \sin\big(\varphi(t)+\alpha(t)\big),\end{cases}$$
$$\tau(t)=\begin{cases}-\sin\big(\varphi(t)+\alpha(t)\big),\\ \cos\big(\varphi(t)+\alpha(t)\big).\end{cases} \tag{53}$$

Similarly, the tangential component of the velocity is found as:

$$v_{Kn}(t)=\dot{\mathbf{r}}_K(t)\cdot\mathbf{n}(t),$$
$$v_{K\tau}(t)=\dot{\mathbf{r}}_K(t)\cdot\tau(t). \tag{54}$$

Let's now turn to the impulsive interaction between the rotating hammer and the bee bread granule. During the interaction, the force acts in a direction that is approximately normal to the local hammer surface.

Let the unit normal vector be oriented along the local radial direction from the rotor center to the contact point. Then the interaction force vector $\vec{n}$ can be represented as

$$\vec{F}_n=F_n\cdot\vec{n}, \tag{55}$$

where $\vec{F}_n$ – the normal impact force, $\vec{n}$ – the normal unit vector, F_n – the scalar magnitude of the force.

According to the impulse-momentum theorem, the change in momentum of the granule in the normal direction is given by

$$m(v_{1n}-v_{0n})=J_n, \tag{56}$$

where J_n – the normal impulse applied over the impact duration Δt, v_{0n}, v_{1n} – the normal velocity components before and after impact, m is the mass of the granule.

The relationship between pre-impact and post-impact normal velocities is established using the coefficient of restitution e

$$v_{1n}=-ev_{0n}, \tag{57}$$

where $e \in [0,1]$ – a phenomenological parameter that describes energy loss during impact. For biological granules, $e \approx 0.6–0.8$ [17, 18].

From equations (56), (57), it is possible to derive the impulse as

$$J_n=m\left(v_{1n}-v_{0n}\right)=-m(1+e)v_{0n}. \tag{58}$$

The change in the granule's tangential velocity due to frictional interaction is computed analogously. Assuming dry friction with coefficient f, the tangential impulse is

$$J_t=-f|J_n|\operatorname{sgn}\left(v_{0\tau}\right), \tag{59}$$

where $J_m = fJ_n$ under Coulomb's law; this impulse changes the tangential velocity component of the granule.

The total change in kinetic energy of the granule due to the impact is expressed as

$$\Delta E=\frac{1}{2}m(v_0^2-v_1^2), \tag{60}$$

where ΔE – the net energy loss; $\vec{v}_0$, $\vec{v}_1$ – the full velocity vectors of the granule before and after contact.

The results demonstrate that for inelastic impacts with $e = 0.7$, the granule loses more than 20% of its kinetic energy in a single interaction, primarily due to deformation and internal damping. These results are consistent with experimental observations for granular plant-based particles [20, 21].

Let's now consider the sequence of four successive impacts of the granule with different hammer elements during its motion inside the rotor. Each impact resets the initial condition for the post-impact motion described by equations (27)–(29).

To model this, it is possible to define a recursive structure for the trajectory segments. Let the i-th impact occur at time t_i, and the corresponding parameters after impact are x_{0i}, φ_{0i}. Then the radial displacement and angular position after each impact are described as

$$x_i(t)=x_{0i}\,e^{-\beta(t-t_i)},\ t\geq t_i, \tag{61}$$

and

$$\varphi_i(t)=\omega(t-t_i)+\varphi_{0i}, \tag{62}$$

where $i = 1, 2, 3, 4$; x_{0i} – the post-impact radial offset; φ_{0i} – the angular reset depending on rotor position at impact.

The parametric trajectory in the stationary coordinate system for each segment is expressed as

$$X_i(t)=\left(R+x_i(t)\right)\cos\varphi_i(t), \tag{63}$$

and

$$Y_i(t)=\left(R+x_i(t)\right)\sin\varphi_i(t), \tag{64}$$

for coordinates $X_i(t)$ and Y_i(t), respectively.

The velocity magnitude for each segment is computed as

$$v_i(t)=\sqrt{\dot{x}_i^2(t)+\omega^2\left(R+x_i(t)\right)^2}, \tag{65}$$

with analogous formulas to equations (33)–(40).

The cumulative kinetic energy loss over four impacts is computed recursively by applying energy loss ratios at each stage, assuming constant restitution e and identical rotor angular velocity ω.

As illustrated in Fig. 5, the granule trajectory forms a multi-spiral pattern, with decreasing amplitude after each impact. The radial distance after the first impact was ≈80 mm, reducing to ≈45 mm after the second, ≈28 mm after the third, and ≈15 mm after the fourth. Energy drops sharply, especially after the first and second impacts, with more than 70% of initial energy dissipated by the third impact.

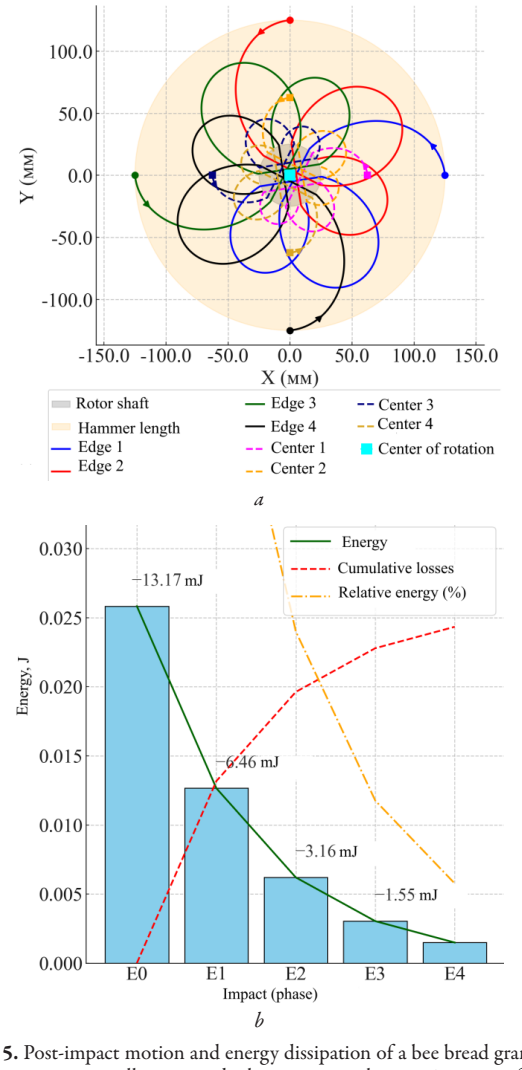

Fig. 5. Post-impact motion and energy dissipation of a bee bread granule during successive collisions inside the rotor: *a* – planar trajectories of the granule projected onto the *OXY* plane for four consecutive impacts; *b* – stepwise decay of the mechanical energy after each impact stage

This modeling result confirms the efficiency of energy attenuation in the rotor system and highlights the self-regulating nature of granule trajectory convergence toward the rotor center.

ISSN-L 2664-9969; E-ISSN 2706-5448

3.3. Discussion

The results of the analytical modeling help to understand the mechanics of bee bread granule impact in a rotary device. The displacement of the granule after the impact follows an exponential decay pattern, which is typical for viscoelastic materials and agrees with the behavior of low-modulus biological materials [3, 5, 6, 17, 19]. The limited elastic restitution is in line with the soft organic systems and biomimetic materials [5, 19]. The trajectory analysis showed a distinct amplitude reduction with each impact, which confirms that the rotor-based system facilitates granule movement towards the rotation axis and prevents rebound or scattering. The damping effect is typical for soft or granular materials in cyclic collision processes [1, 4, 9, 19, 20]. The energy decay and trajectory stabilization pattern agrees with DEM simulations of particle flow in rotary and hammer machines [10, 11, 13]. The optimal hammer mass range was found, beyond which the increase in mass reduces the efficiency of energy transfer due to increased inelastic deformation. Similar results were obtained in rotary impact simulations, where the use of lighter impactors resulted in better preservation of product integrity [10, 12, 15, 19]. These data are in line with previous studies on granule separation and agricultural material processing [7, 8, 14]. The data obtained have significant practical applications for the design of energy-efficient rotary devices for granule separation. Based on the equations obtained, engineers can simulate granule behavior at different rotor speeds and optimize hammer mass, angle of rotation, and surface elasticity for maximum efficiency [14, 21–24]. The model can also be used for the development of predictive control algorithms for automated separation devices [20, 22, 23]. Limitations of the model include the assumption of planar motion and constant material properties, which do not accurately represent the effects of moisture and inhomogeneity on impact dynamics [16, 18, 19]. Future research will generalize the model to three-dimensional motion, time-varying restitution coefficients, and experimental verification using high-speed imaging and DEM analysis [1, 9–11]. These advances will improve the understanding of granular mechanics and facilitate the development of sophisticated rotary separators for biological materials.

4. Conclusions

1. Analytical relationships describing the post-impact motion, velocity, and trajectory of a bee bread granule in a rotary separator were obtained. It was established that the granule motion has a strongly damped character. In particular, for an initial displacement of 80 mm, the amplitude decreases by more than 60% within the first 0.02 s and by more than 80% within 0.05 s. The radial coordinate decreases from approximately 80 mm to less than 20 mm over the same time interval. This confirms rapid attenuation of motion and stabilization of the granule trajectory due to dissipative effects associated with friction and internal damping.

2. The influence of impact parameters and rotor operating conditions on energy dissipation and granule motion was determined. It was found that the efficiency of energy transfer depends strongly on hammer mass and equals approximately 0.7–0.8% for a hammer mass of 5 g, decreases to about 0.1% at 100 g, and falls below 0.05% at 200 g. In addition, during successive impacts, the radial displacement decreases from about 80 mm after the first impact to approximately 15 mm after the fourth impact, with more than 70% of the initial mechanical energy dissipated. These results demonstrate the dominant role of inelastic deformation and friction in the energy dissipation process and provide a quantitative basis for selecting rational rotor parameters.

Acknowledgements

The authors express their sincere gratitude to Volodymyr Ivanovych Rudenko, Director of AVV-100 LLC, one of the oldest enterprises in the Kharkiv region specializing in the manufacture of beekeeping equipment and tools, for facilitating the implementation of the research results under industrial conditions, for providing professional consultations, and for participating in the practical validation of the developed technical solutions.

Conflict of interest

The authors declare that they have no conflict of interest regarding this research, including any financial, personal, authorship, or other relationships that could have influenced the research and the results presented in this article.

Financing

This research was conducted without any external financial support.

Data availability

The data will be provided upon reasonable request.

Use of artificial intelligence

The authors confirm that no artificial intelligence technologies were used in the preparation of this work.

Authors' contributions

Yurii Syromiatnykov: Conceptualization, Methodology, Formal analysis, Investigation, Visualization, Writing – original draft, Writing – review and editing, Supervision, Project administration; ***Oleksandr Bielykh:*** Methodology, Formal analysis, Investigation, Validation, Data curation, Visualization, Writing – review and editing; ***Oleksandr Kharchenko***: Formal analysis, Investigation, Validation, Data curation, Writing – review and editing.

References

1. Ghazi Alshanti, W. (2019). Discrete Element Modeling of a Projectile Impacting and Penetrating into Granular Systems. *Ballistics.* IntechOpen. https:// /10.5772/intechopen.75550
2. Chou, Y. F., Keh, H. J. (2024). Axisymmetric Slow Rotation of Coaxial Soft/Porous Spheres. *Molecules, 29 (15),* 3573. https://doi.org/10.3390/molecules29153573
3. Sanoria, M., Chelakkot, R., Nandi, A. (2021). Influence of interaction softness on phase separation of active particles. *Physical Review E, 103 (5).* https://doi.org/10.1103/physreve.103.052605
4. Lips, D., Cereceda-López, E., Ortiz-Ambriz, A., Tierno, P., Ryabov, A., Maass, P. (2022). Hydrodynamic interactions hinder transport of flow-driven colloidal particles. *Soft Matter, 18 (47),* 8983–8994. https://doi.org/10.1039/d2sm01114j
5. Zhou, L., Ren, L., Chen, Y., Niu, S., Han, Z., Ren, L. (2021). Bio-Inspired Soft Grippers Based on Impactive Gripping. *Advanced Science, 8 (9).* https://doi.org/10.1002/advs.202002017
6. Seifert, J., Koch, K., Hess, M., Schmidt, A. M. (2020). Magneto-mechanical coupling of single domain particles in soft matter systems. *Physical Sciences Reviews, 7 (11),* 1237–1261. https://doi.org/10.1515/psr-2019-0092
7. Rosas, A., Buceta, J., Lindenberg, K. (2003). Dynamics of two granules. *Physical Review E, 68 (2).* https://doi.org/10.1103/physreve.68.021303
8. van der Meer, D. (2017). Impact on Granular Beds. *Annual Review of Fluid Mechanics, 49 (1),* 463–484. https://doi.org/10.1146/annurev-fluid-010816-060213
9. Sano, T. G., Kanazawa, K., Hayakawa, H. (2016). Granular rotor as a probe for a nonequilibrium bath. *Physical Review E, 94 (3).* https://doi.org/10.1103/physreve.94.032910
10. Wang, X., Huang, Y., Zhang, F., Meng, Q. (2025). Influence of Rotor-Induced Airflow on Particle Fragmentation in an Impact Crusher: A Computational Fluid Dynamics–Discrete Element Method Study. *ACS Omega, 10 (39),* 46051–46064. https://doi.org/10.1021/acsomega.5c06659

11. Ghodki, B. M., Chhetri, K. B., Goswami, T. K. (2020). Numerical modeling of granular flow in star valve type cryogenic precooler. *Journal of Food Process Engineering, 43 (4).* https://doi.org/10.1111/jfpe.13376
12. Yang, J. H., Fang, H. Y., Luo, M. (2015). Load and wear experiments on the impact hammer of a vertical shaft impact crusher. *IOP Conference Series: Materials Science and Engineering, 103.* https://doi.org/10.1088/1757-899x/103/1/012041
13. Feng, F., Shi, J., Yang, J., Ma, J. (2020). Study on Wear form of Split Cone of Vertical Shaft Impact Crusher. *Journal of Scientific Research and Reports, 21 (11),* 13–20. https://doi.org/10.9734/jsrr/2020/v26i1130331
14. Xu, B., Cui, Q., Guo, L., Hao, L. (2024). Design and Parameter Optimization of a Combined Rotor and Lining Plate Crushing Organic Fertilizer Spreader. *Agronomy, 14 (8),* 1732. https://doi.org/10.3390/agronomy14081732
15. Paraschiv, G., Moiceanu, G., Voicu, G., Chitoiu, M., Cardei, P., Dinca, M. N., Tudor, P. (2021). Optimization Issues of a Hammer Mill Working Process Using Statistical Modelling. *Sustainability, 13 (2),* 973. https://doi.org/10.3390/su13020973
16. Kim, A. S., Kim, H.-J. (2017). Dissipative Dynamics of Granular Materials. *Granular Materials.* IntechOpen. https://doi.org/10.5772/intechopen.69196
17. Kollmer, J. E., Sack, A., Heckel, M., Pöschel, T. (2013). Relaxation of a spring with an attached granular damper. *New Journal of Physics, 15 (9),* 093023. https://doi.org/10.1088/1367-2630/15/9/093023
18. Păun, A., Stroescu, G., Milea, D., Olan, M., Epure, M. (2019). Concaves influence on the milling process of cereal seeds in hammer mills. *E3S Web of Conferences, 112,* 03009. https://doi.org/10.1051/e3sconf/201911203009
19. Ahmadian, H., Ghadiri, M. (2021). Granule attrition by coupled particle impact and shearing. *Advanced Powder Technology, 32 (1),* 204–210. https://doi.org/10.1016/j.apt.2020.12.001
20. Li, T., Shi, G., Zhang, Q. (2024). Research on hammering characteristics of hammer mill based on discrete element method. *Engineering Research Express, 6 (3),* 035540. https://doi.org/10.1088/2631-8695/ad6ca4
21. Kyzas, G., Mitropoulos, A. C. (Eds.) (2018). *Granularity in Materials Science.* IntechOpen. https://doi.org/10.5772/intechopen.75231
22. Syromyatnikov, Y. N., Orekhovskaya, A. A., Dzjasheev, A.-M. S., Tikhonov, E. A., Kalimullin, M. N., Ivanov, A. A., Sokolova, V. A. (2021). Improving stability of movement of machine section for soil preparation and seeding. *Journal of Physics: Conference Series, 2094 (4),* 042027. https://doi.org/10.1088/1742-6596/2094/4/042027
23. Pashchenko, V. F., Syromyatnikov, Y. U. N. (2019). The transporting ability of the rotor of the soil-cultivating loosening and separating vehicle. *Traktory i Sel Hozmashiny, 86 (2),* 67–74. https://doi.org/10.31992/0321-4443-2019-2-67-74
24. Syromyatnikov, Y. N., Orekhovskaya, A. A., Dzjasheev, A.-M. S., Kalimullin, M. N., Tikhonov, E. A., Luchinovich, A. A., Bielykh, A. V. (2021). Cultivator points of the rotary tillage loosening and separating machine of the stratifier. *Journal of Physics: Conference Series, 2094 (4),* 042024. https://doi.org/10.1088/1742-6596/2094/4/042024

Yurii Syromiatnykov, *PhD, Assistant, Department of Agroengineering, State Biotechnological University, Kharkiv, Ukraine, ORCID: https://orcid.org/0000-0001-9502-626X*

✉ ***Oleksandr Bielykh,*** *PhD Student, Department of Agroengineering, State Biotechnological University, Kharkiv, Ukraine, e-mail: sashafincol@gmail.com, ORCID: https://orcid.org/0009-0007-5490-4098*

Oleksandr Kharchenko, *PhD Student, Department of Agroengineering, State Biotechnological University, Kharkiv, Ukraine, ORCID: https://orcid.org/0009-0009-4955-3478*

✉ *Corresponding author*